Supplementary Information

Quantifying cell-generated mechanical forces within living embryonic tissues

Otger Campàs, Tadanori Mammoto, Sean Hasso, Ralph A. Sperling, Daniel O' Connell, Ashley G. Bischof, Richard Maas, David A. Weitz, L. Mahadevan & Donald E. Ingber

Supplementary Figure 1:

Adhesion of cells on functionalized droplets. A detailed description of Supplementary Figure 1 is provided in the Online Methods (see 'Adhesion of cells on functionalized droplets').

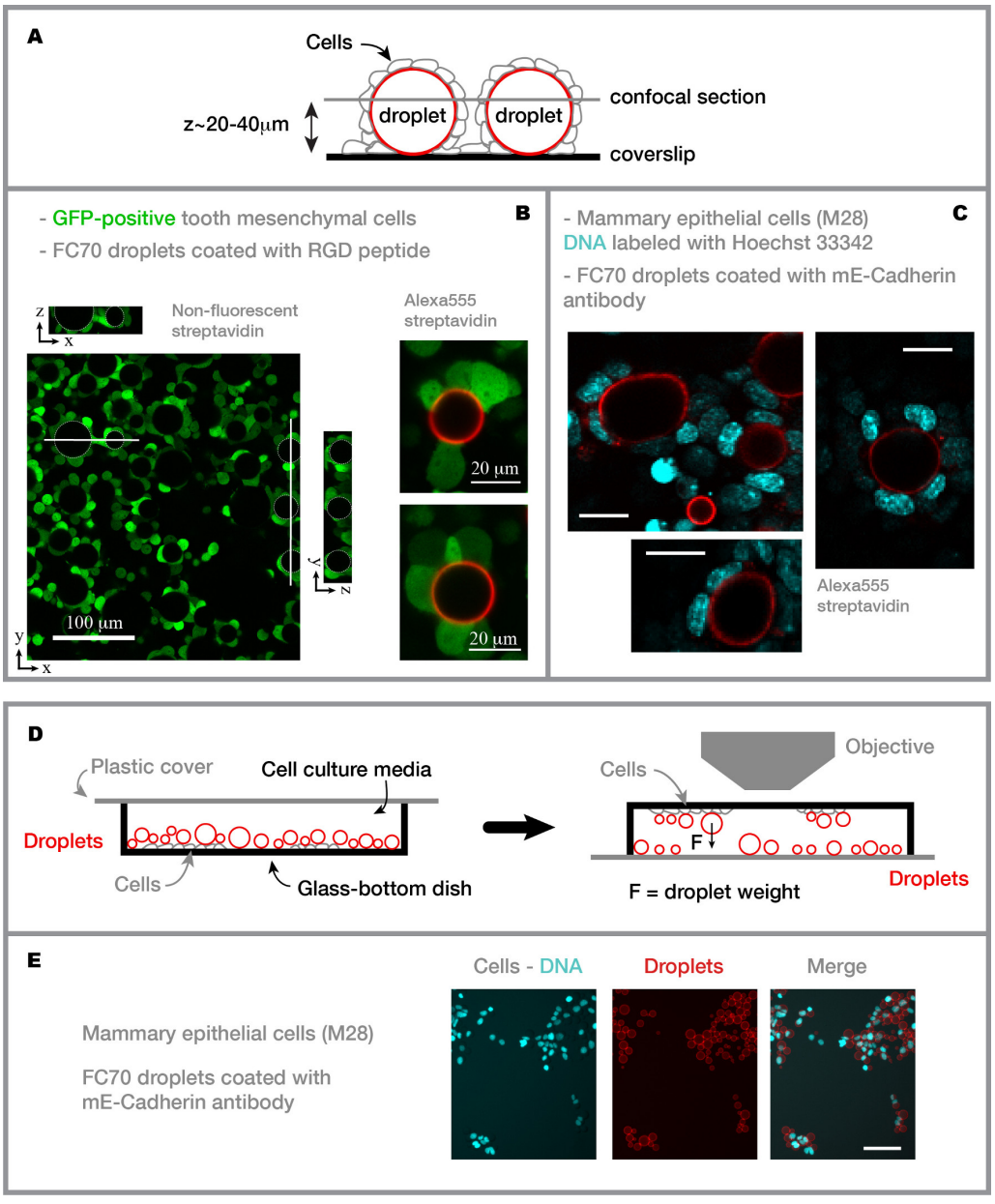

Supplementary Figure 2:

Image Analysis. A detailed description of Supplementary Figure 2 is provided in the Online Methods (see 'Image analysis').

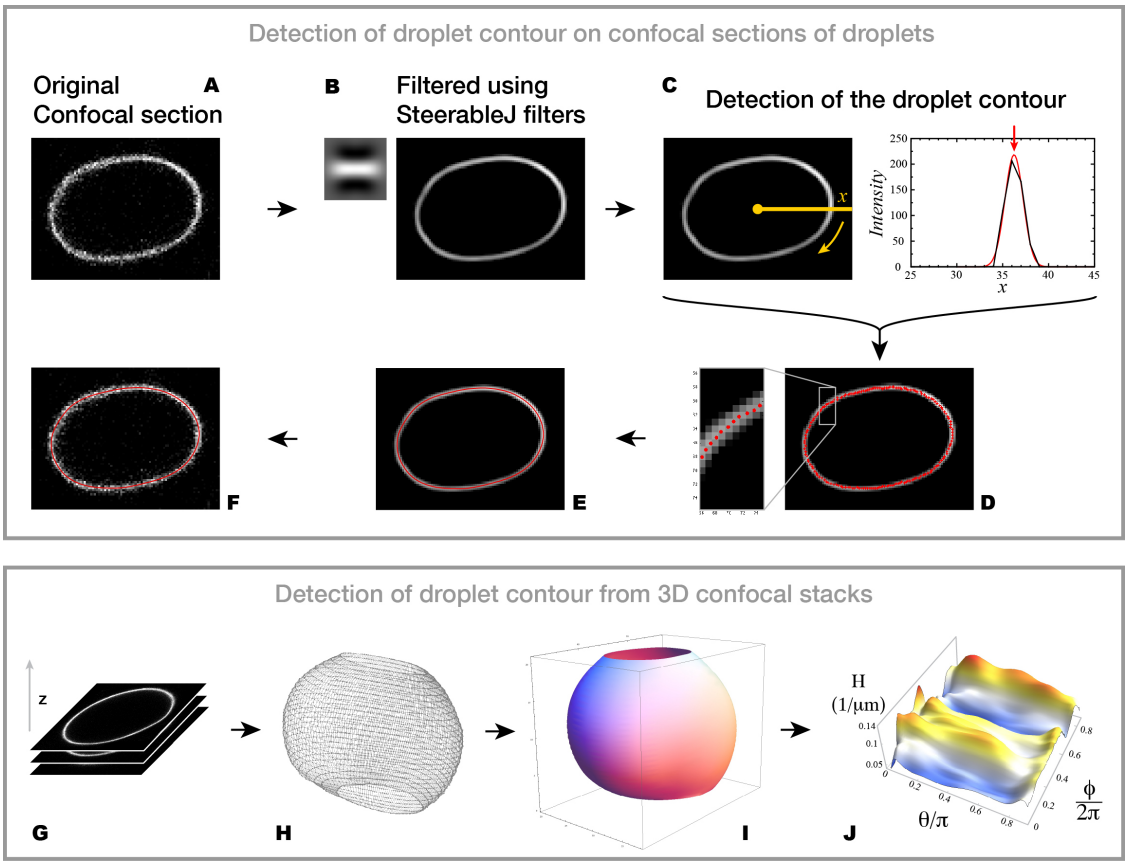

Supplementary Note 1:

Measure of cell size in cultured cellular aggregates and living mouse mandibles

This Supporting Information explains the methods used to measure the cell size both in cultured cellular aggregates and living mouse mandibles.

Measure of cell size in cultured aggregates of mammary epithelial cells

In order to measure cell size in aggregates of mammary epithelial (M28) cells, we incubated cell aggregates with cell culture media (DMEM supplemented with 10% FBS and 1% PenStrep) containing the DNA dye Hoechst 33342 (Invitrogen) at a concentration of $3\,\mu$M. The aggregates were incubated for about 12 hours to allow the dye to penetrate within the aggregates. We then imaged the aggregates as explained in the Methods section and measured the distance d between nearest neighbor nuclei (Fig. 1A,B). For these measurement we only used nuclei from nearest neighboring cells that appear to be in the same focal plane. These measurements allowed us to obtain the distribution of the distance d between nearest neighbor nuclei (Fig. 1C). The average cellular size corresponds to the average distance between nearest neighbor nuclei, which is obtained directly from the distribution of d to be $12 \pm 2\,\mu$m.

Measure of cell size in cultured aggregates of tooth mesenchymal cells

Cellular aggregates of GFP-positive tooth mesenchymal cells allow a direct measure of cellular size as the fluorescent levants for each cell differ slightly, allowing a direct identification of the cell contour (Fig. 1D). Tooth mesenchymal cells in dense aggregates tend to acquire an oblate shape with long and short axes, b and a respectively (Fig. 1D,E). We measured cellular size along both axis and obtained their corresponding distributions (Fig. 1G). The size of the cell along its longest axis shows a wide distribution, indicating a large variation in cellular sizes. The average cellular sizes along the short and long axis were obtained from their corresponding distributions to be $10 \pm 3\,\mu$m and $24 \pm 4\,\mu$m respectively. Cells were never observed to contact droplets along the short axis. Instead, their long axis was essentially perpendicular to the droplet normal at the contact point. The fact that the maximal relative droplet deformations occur at a length scale of $23\,\mu$m (Fig. 3F of the main text), essentially the same as the average cell size along their long axis, and that the relative droplet deformations are spread over a wide range of length scales (Fig. 3F of the main text), similar to the spread of cell sizes along both axes, indicates that the mechanical inhomogeneities in the cell aggregate are dominated by the largest cellular sizes.

Measure of cell size in living mouse mandibles

The average size of tooth mesenchymal cells in the dental mesenchyme of mouse mandibles was measured in two different ways. First, dissected mouse mandibles were incubated for 7 hours in culture media (as described in the Methods section) containing the DNA dye Hoechst 33342 (Invitrogen) at a concentration of $3\,\mu$M. The distance d between nearest neighbor nuclei was

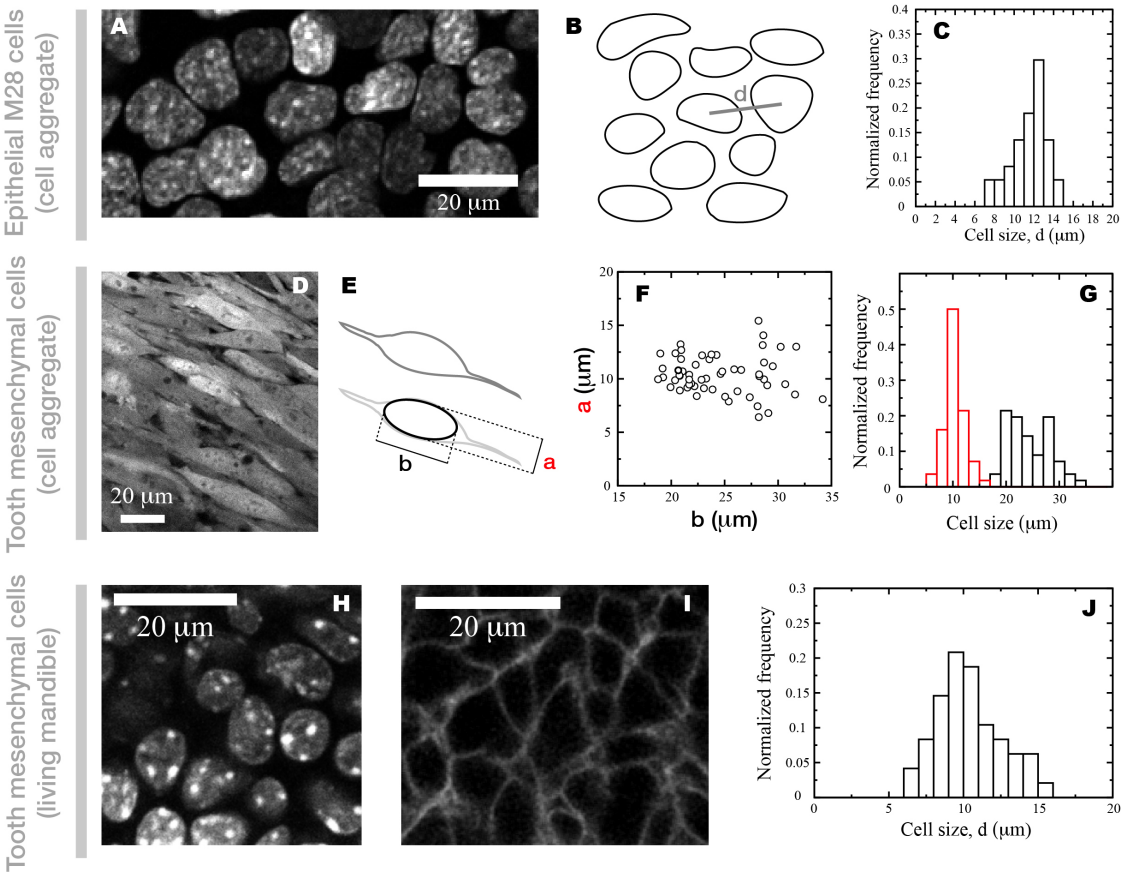

Figure 1: **Distribution of cellular sizes in cultured aggregates of mammary epithelial cells and tooth mesenchymal cells, and in living mandibles.** (A-C) Measure of cellular sizes in aggregates of mammary epithelial cells. (A) Confocal section through an aggregate of DNA-labeled mammary epithelial cells. (B) Sketch of the nuclei in the aggregate with the definition of the distance d between nearest neighbor nuclei. (C) Distribution of d. (D-G) Measure of cellular sizes in aggregates of GFP-positive tooth mesenchymal cells. (D) Confocal section through an aggregate. (E) Sketch of the typical oblate cell shape and the definition of the lent and short axes, b and a respectively. (F) Measured values of a and b. (G) Distributions of a and b. (H-J) Measure of cellular sizes in the dental mesenchyme of tooth mandibles at developmental stage E11. (H) Confocal section through the dental mesenchyme of a DNA-labeled mandible. (I) Confocal section of the dental mesenchyme of a mandible with a fluorescent membrane reporter for tooth mesenchymal cells. (J) Distribution of tooth mesenchymal cell sizes in the dental mesenchyme of mouse mandibles.

measured as described above for mammary epithelial cells (Fig. 1H and Fig. 1B). The obtained distribution for distance d between nearest neighbor nuclei is shown in Fig. 1J. The average cellular size corresponds to the average distance between nearest neighbor nuclei, which is obtained directly from the distribution of d to be $10 \pm 2\,\mu$m. We further checked the value of the average cellular size by estimating the size of tooth mesenchymal cells in mouse mandibles with fluorescent membrane reporters (Fig. 1I).

Supplementary Note 2:

Measure of droplet interfacial tension

This Supporting Information details the measurements of the interfacial tension between FC70 oil, coated as described in the main text, and the cell/tissue culture media.

The interfacial tension was measured using the Du Noüy ring technique (Sigma 700, Biolin Scientific). All experiments were conducted at room temperature if not stated otherwise. Surface and interfacial tension were measured over time to make sure equilibrium values were measured. All the standard deviations provided for the surface/interfacial tensions values correspond to statistics on 5 different samples. First, filtered FC70 was poured into an open glass container creating an FC70 surface exposed to air, and the surface tension of FC70 was measured to be 18 ± 2 mN/m (Fig. 2A), which coincides with the surface tension value (18 mN/m) provided by the vendor (3M Co.). Then, we carefully poured purified, deionized water on the top of the FC70 oil layer. As FC70 is nearly twice as dense as water (FC70 density is 1970 kg/m^3), the poured water created a layer of top of FC70. We then measured the interfacial tension of FC70 and purified water to be 46 ± 2 mN/m (Fig. 2B). We then carefully pipetted out the water layer and proceeded to measure the interfacial tension at every step of the oil coating (functionalization) procedure described in the Methods section. We carefully pipetted out the water layer on top of FC70 and substituted with a water solution containing DSPE-PEG2000-biotin surfactants at a concentration of 0.2 mM. The interfacial tension in this case was measured to be 32 ± 2 mN/m (Fig. 2C). The DSPE-PEG2000-biotin solution was almost completely removed and purified water was added and subsequently removed 3 times, leaving only a DSPE-PEG2000-biotin layer at the FC70-water interface. The interfacial tension of the FC70-water interface with the DSPE-PEG2000-biotin surfactant layer was measured to be 35 ± 2 mN/m (Fig. 2D), slightly larger than the previous measurement due to desorption of some of the surfactant. We then substituted the water layer with a water solution containing fluorescent streptavidin (FITC-streptavin) at a concentration of 1 μM. This concentration and the volume of solution used (50 mL) ensured a large excess of streptavidin molecules to quickly, and fully, coat the surface. The interfacial tension in this case remained unchanged (35 ± 2 mN/m). The fluorescent streptavidin solution was almost completely removed and purified water was added and subsequently removed 3 times, leaving only a DSPE-PEG2000-biotin:streptavidin(FITC) layer at the FC70-water interface, which appeared colored thanks to the high concentration of fluorescent streptavidin at the interface. We then carefully substituted the water layer on top of the DSPE-PEG2000-biotin:streptavidin(FITC) coated FC70 layer with the cell/tissue culture media used in the experiments described in the main text (DMEM supplemented with 10% FBS and 1% PenStrep; see Online Methods). While in all previous steps the interfacial tension reached a constant value in less than a minute, when cell/tissue culture media was added, the interfacial tension took about 40 minutes to equilibrate, as indicated by the time evolution of the interfacial tension (Fig. 2E). This is due to the fact that several chemical species (mainly BSA proteins, a large component of FBS) adsorb on the interface, lowering the interfacial tension. The equilibrium interfacial tension of the DSPE-PEG2000-biotin:streptavidin(FITC) coated FC70 with the cell/tissue culture media was measured to be 27 ± 2 mN/m (Fig. 2E). We then changed the temperature of the system to 37°C by putting it in contact with a thermal bath at this temperature,

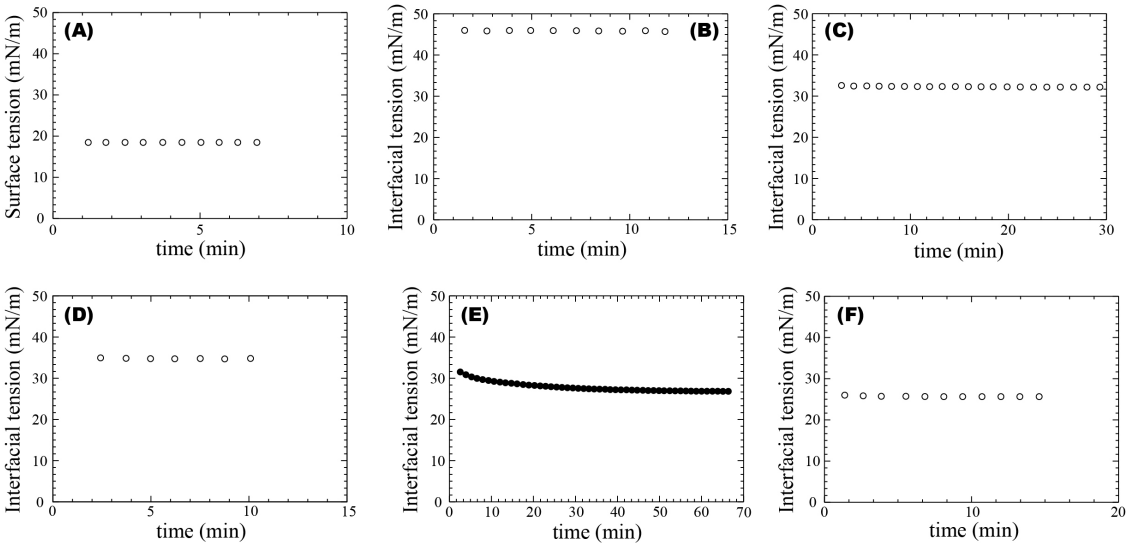

Figure 2: **Time dependence of the surface/interfacial tension of FC70 oil at each step of the coating (functionalization) process.** (A) Surface tension of the FC70-air surface. (B) Interfacial tension of FC70 and purified water. (C) Interfacial tension of FC70 and a water solution containing DSPE-PEG2000-biotin surfactants at a concentration of 0.2 mM. The recordings of the interfacial tension started about two minutes after addition of the DSPE-PEG2000-biotin solution. (D) Interfacial tension of FC70 containing a surface layer of DSPE-PEG2000-biotin surfactants with a water solution containing fluorescent streptavidin (FITC-streptavin) at a concentration of 1 μM. (E) Interfacial tension of FC70 containing a surface layer of DSPE-PEG2000-biotin:streptavidin(FITC) with cell/tissue culture media at room temperature. The interfacial tension diminishes over time until it reaches its equilibrium value. (F) Interfacial tension of the result in step at a temperature of 37°C.

and measured the interfacial tension at this temperature to be 26 ± 2 mN/m (Fig. 2F).

Due to limitations in the quantity of available Krytox-DDA diblocks, the interfacial tension of FC70 containing Krytox-DDA diblocks, coated as described above and in the Methods section, was measured using the pendant drop method because it required a much smaller quantity of reagents for the measurement. For these measurements, we used a custom-built pendant drop apparatus. In order to check that we were able to measure meaningful values of interfacial tensions, we first measured already known values of interfacial tensions in the absence of Krytox-DDA diblocks.The interfacial tension of FC70 and purified water was measured to be 49 ± 3 mN/m, and the interfacial tension of FC70 with a water solution containing DSPE-PEG2000-biotin surfactants at a concentration of 0.2 mM was measured to be 31 ± 3 mN/m. Therefore, the values of the interfacial tension measured with the pendant drop apparatus agree within the experimental error with the values measured using the Du Noüy ring technique. In order to check if the Krytox-DDA diblocks were functional, we measured the interfacial tension of FC70 containing Krytox-DDA diblocks at a 1% w/w concentration with a water solution containing DSPE-PEG2000-biotin surfactants at a concentration of 0.2 mM. It is expected that the DDA block will interact with the DSPE hydrocarbon tail, thereby stabilizing further the DSPE-PEG2000-biotin surfactants on the interface thanks to the Krytox block (Fig. 1 of the main text). The interfacial tension of a droplet of FC70 containing Krytox-DDA diblocks at a 1% w/w concentration with a water solution containing DSPE-PEG2000-biotin surfactants at a concentration of 0.2 mM, was measured to be 14 ± 3 mN/m. This value is substantially smaller than in the absence of Krytox-DDA diblocks, indicating that the diblocks are active and stabilize further the DSPE-PEG2000-biotin surfactants at the interface. Finally, the interfacial tension of FC70 containing Krytox-DDA diblocks at a 1% w/w concentration and coated with DSPE-PEG2000-biotin:streptavidin(FITC) with cell/tissue culture media at 37°C was measured to be 4 ± 3 mN/m.

Supplementary Note 3:

Measure of isotropic stresses using microdroplets partially embedded in living tissue

In this Supporting Information we describe how to measure the total normal stresses on a microdroplet (both isotropic and anisotropic contributions) using droplets that are only partially surrounded by cells. While in most of our experiments microdroplets are fully surrounded by cells, in some rare cases microdroplets where positioned in the dental epithelium and had a cell-free portion of the droplet (Fig. 3). The cell-free region of the droplet surface takes the shape of a spherical cup (Fig. 3C), in agreement with Laplace's Law in absence of applied external normal stresses. Writing Laplace's Law in the cell-free spherical cup we obtain [1, 2]

$$p_i = p_e + \frac{2\gamma}{R_c} \, , \tag{1}$$

where p_i is the internal hydrostatic pressure of the droplet, p_e is the hydrostatic pressure of the surrounding fluid (culture media) and R_c is the radius of curvature of the cell-free spherical cup. In regions of the droplet surface surrounded by cells, i.e., where cells are applying local normal stresses σ_{nn}, Laplace's Law reads

$$p_i = p_e + 2\gamma \mathrm{H} - \sigma_{nn} \, , \tag{2}$$

where H is the local mean curvature of the droplet surface. Combining Eqs. 1 and 2, we obtain

$$\sigma_{nn} = 2\gamma \left(\mathrm{H} - 1/R_c \right) \, , \tag{3}$$

indicating that cells are pulling on the droplet ($\sigma_{nn} > 0$) in regions with mean curvature $\mathrm{H} > 1/R_c$ and pushing of the droplet surface in regions where $\mathrm{H} < 1/R_c$. Decomposing the normal stress σ_{nn} in its isotropic and anisotropic components, namely $\sigma_{nn} = -P_i + \delta\sigma_{nn}$, and knowing that $\delta\sigma_{nn} = 2\gamma \left(\mathrm{H} - 1/R \right)$ (with R being the radius of the droplet in its undeformed spherical state; see main text), the isotropic component of the normal stresses reads

$$P_i = 2\gamma \left(\frac{1}{R_c} - \frac{1}{R} \right) \, . \tag{4}$$

Fig. 3A,B shows a DIC image of a droplet (coated with ligands for integrin receptors) partially embedded in the dental epithelium of a mouse mandible at stage E11. A portion of the droplet surface, characterized by a spherical cup shape (Fig. 3C,D), is free of cells and in direct contact with the tissue culture media. While DIC images do not allow a careful 3D reconstruction of the droplet shape, we can still measure the curvature of the cell-free spherical cup to be $R_c \simeq 13 \pm 2 \, \mu$m (Fig. 3C,D). Although the radius R of the undeformed spherical state of the droplet cannot be measured from the DIC images (a full 3D reconstruction of the droplet shape would be needed), it is clear that $R > R_c$ (Fig. 3C,D). From Eq. 4 we can then see that the maximal value possible for the isotropic component of the normal stress is 0.6 ± 0.4 nN/μm^2 ($\gamma \simeq 4 \pm 3$ mN/m), corresponding to a radius $R >> R_c$, so that $P_i \leq 0.6 \pm 0.4$ nN/μm^2 for this particular droplet.

It is also possible to measure the in-plane curvature κ_i at different points of the droplet surface from Fig. 3C, and estimate the out-of-plane curvature κ_o of the droplet surface at those points using DIC images in neighboring z-planes. Using Eq. 3 and knowing that $H = (\kappa_i + \kappa_o)/2$, we obtain the normal stresses at points a and b on the droplet surface to be $\sigma_{nn} \simeq 2.2 \pm 1.6\,\mathrm{nN}/\mu\mathrm{m}^2$ and $\sigma_{nn} \simeq -0.3 \pm 0.2\,\mathrm{nN}/\mu\mathrm{m}^2$, respectively, indicating that cells are pulling the droplet at point a and pushing it at point b.

Despite the considerable error in the previous measures and the fact that this situation cannot be directly compared to the results in the main text, our results indicate that the value of the isotropic component of the stress obtained above is similar to the measured values of the anisotropic stresses.

References

[1] Boukellal, H., Campas, O., Joanny, J.-F., Prost, J. & Sykes, C. Soft Listeria: actin-based propulsion of liquid drops.

[2] De Gennes, P.-G., Brochard-Wyart, F. & Quere, D. Capillarity and Wetting Phenomena: Drops, Bubbles, Pearls, Waves. Springer (2003).

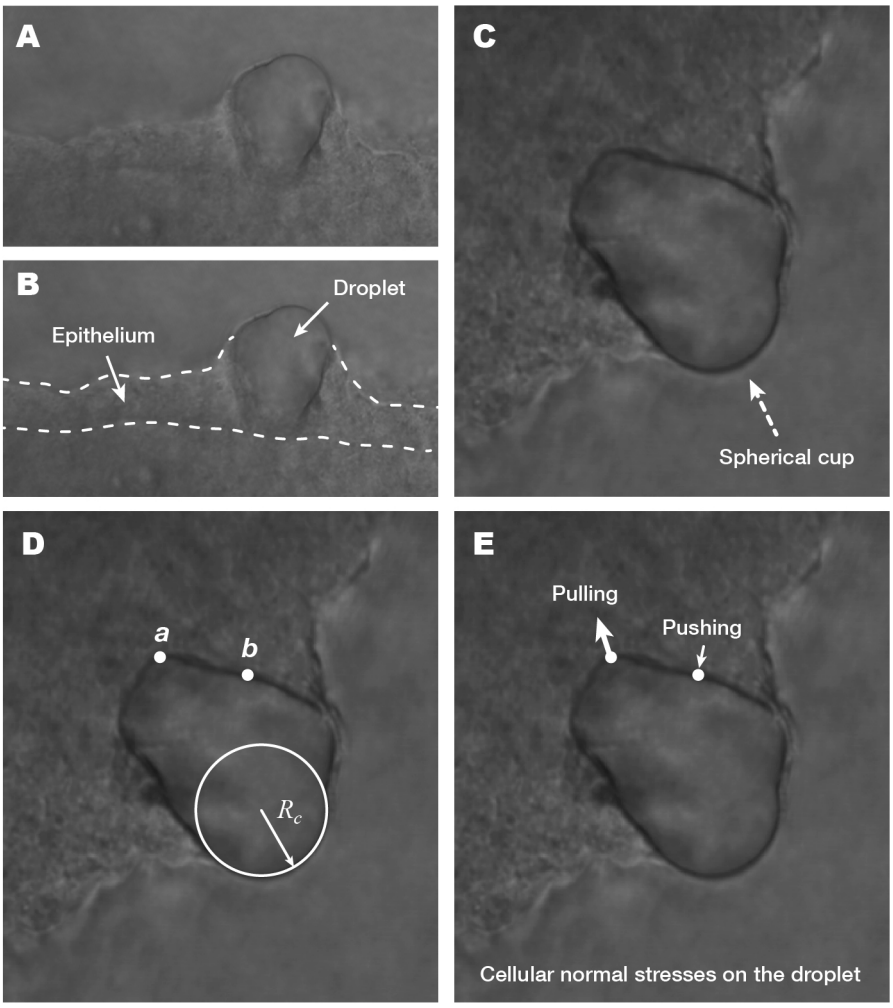

Figure 3: **Measure of total normal stresses (isotropic + anisotropic components) applied by cells on a microdroplet only partially embedded in tissue.** (A) Differential Interference Contrast (DIC) image of a droplet partially embedded in the dental epithelium of a mouse mandible at stage E11. The droplet was coated with ligands (RGD peptide) for integrin receptors on the cell surface. (B) Same as in A, but with dashed lines indicating the borders of the epithelial tissue obtained from observation of the tissue morphological features. The location of the droplet is also indicated. (C) Image of an oblique plane going through the droplet obtained from a 3D stack of DIC images. The cell-free spherical cup can be easily observed. (D) Same as C, but indicating the points a and b where stresses are calculated (see text and panel E) as well as the radius of curvature R_c of the spherical cup. (E) Same as C, with arrows indicating the direction of the local normal stresses applied by cells at points a and b.